THE ASTROPHYSICAL JOURNAL, 358:L49–L52, 1990 August 1

DETECTION OF AN ISOTOPIC SHORT SUBMILLIMETER CO LINE: COLUMN DENSITIES OF WARM GAS IN MOLECULAR CLOUDS

U. U. GRAF,[1] R. GENZEL,[1] A. I. HARRIS,[1] R. E. HILLS,[2] A. P. G. RUSSELL,[1,3] AND J. STUTZKI[1]
Received 1990 March 28; accepted 1990 May 9

ABSTRACT

We report the first astronomical detection of isotopic ^{13}CO $J = 6 \rightarrow 5$ emission at 661 GHz from the molecular clouds in Orion A and in NGC 2024. Strong lines (Rayleigh-Jeans main-beam brightness temperature ≈ 50 K) indicate large column densities of warm, dense, molecular gas in these star formation regions. From the new ^{13}CO data, together with complementary ^{13}CO $J = 3 \rightarrow 2$ and ^{12}CO $J = 6 \rightarrow 5$ measurements, we estimate that H_2 column densities of gas with temperature ≥ 100 K lie between 3×10^{22} and 4×10^{23} cm^{-2}. These column densities, corresponding to $\geq 30\%$ of the total molecular gas mass in the observed star-forming regions, are difficult to explain by present theoretical heating models. In NGC 2024 and the Orion Bar, where lines are narrow ($\Delta v_{LSR} \leq 3$ km s^{-1}), shock heating is very unlikely. The correlation of warm CO column density with UV intensity, also indicated by the nondetection ($T_{mb} < 10$ K) of ^{13}CO $J = 6 \rightarrow 5$ emission toward the weak UV source NGC 2023, favors heating by UV radiation. However, present photodissociation region (PDR) models fail to predict the large quantities of warm gas detected in NGC 2024 and in the Orion Bar.

Subject headings: interstellar: matter — interstellar: molecules — nebulae: individual (Orion A, NGC 2024)

I. INTRODUCTION

Submillimeter and far-infrared observations of carbon monoxide (CO) (Jaffe, Harris, and Genzel 1987; Harris *et al.* 1987*b*; Genzel, Poglitsch, and Stacey 1988; Schmid-Burgk *et al.* 1989; Boreiko, Betz, and Zmuidzinas 1989) have indicated the presence of warm, dense molecular gas near regions of recent star-forming activity. Estimates based on the brightness temperature ratio between mid-J submillimeter ^{12}CO and high-J (far-IR) ^{12}CO lines in M17 and S106 (Harris *et al.* 1987*b*) gave a lower limit of $\approx 10^{18}$ cm^{-2} [$\tau(^{12}CO\ 7 \rightarrow 6) \approx 1$] to the CO column density of quiescent ($\Delta v \leq 10$ km s^{-1}) gas at temperatures of at least 100 K and H_2 densities of 10^4–10^6 cm^{-3}. This lower limit corresponds to between 5% and 20% of the gas mass in these regions. The mid-J ^{12}CO lines are likely to be optically thick in most sources. In order to obtain a better estimate of the column densities, it is thus of great interest to observe isotopic mid-J CO lines, which are likely to be optically thin.

II. OBSERVATIONS AND RESULTS

The ^{13}CO $J = 6 \rightarrow 5$ (661.0673 GHz; 453.5 μm [calculated from molecular constants given by Lovas and Krupenie 1974]) detection was made on 1989 November 27 with the MPE cooled Schottky submillimeter heterodyne receiver (Harris *et al.* 1987*a*) mounted at the Nasmyth focus of the James Clerk Maxwell Telescope (JCMT), on Mauna Kea, Hawaii. The local oscillator laser line we used is the 670.4628 GHz lines of CH_3I (Dyubko *et al.* 1975; Arimondo 1984). The receiver temperature measured at the telescope was 3500 K (DSB).

The data were calibrated in the way described by Harris (1986) and Harris *et al.* (1987*b*). Scans across the limb of Jupiter (44″ diameter) indicate that the telescope beam is a composite of a diffraction-limited beam of 8″ FWHM and a pedestal of $\approx 40''$ FWHM due to errors in the telescope surface and possibly nonperfect focusing. The on-axis amplitude ratio of the 8″ component to the 40″ component is 85/15. The corresponding power ratio is 20/80. All line temperatures listed below are on a Rayleigh-Jeans main-beam brightness temperature scale, that is, antenna temperatures corrected for atmospheric absorption and main-beam efficiency. Main-beam efficiencies determined for this composite beam on the Moon and on Jupiter are 37% and 32%, respectively. In addition, the temperatures given below include a source coupling efficiency correction of 65%, which is appropriate for a uniform source of Jupiter size. For larger sources, like the Orion spike source, this value thus leads to a slight overestimate of the true main-beam brightness temperature, whereas in smaller sources (Orion plateau), it tends to underestimate it. Pointing and focus were frequently checked with the UKT 14 bolometer. We estimate that the pointing accuracy is better than $\pm 5''$.

Complementary ^{12}CO $J = 6 \rightarrow 5$ and ^{13}CO $J = 3 \rightarrow 2$ observations were obtained between 1989 November 27 and December 18. The ^{12}CO $J = 6 \rightarrow 5$ line (690.473 GHz) was observed with the MPE receiver, using the 692.951 GHz transition of HCOOH (Dyubko, Svich, and Fesenko 1975) as local oscillator line. For the ^{13}CO $J = 3 \rightarrow 2$ line, we used the JCMT 350 GHz facility receiver. The beam size at this frequency is 15″ FWHM; the main-beam efficiency measured on Jupiter is 50%. In addition to the observatory's standard calibration procedure, we applied corrections for sideband imbalance because of the strong atmospheric absorption feature at 325 GHz. We estimate the uncertainty in the absolute line intensities to be about $\pm 30\%$. The calibration error on line ratios is smaller because systematic errors like the uncertainty of the Jupiter temperature cancel out.

Strong ^{13}CO $J = 6 \rightarrow 5$ emission was detected from a number of positions toward Orion IRc2 (Fig. 1*a*), Θ^1C, the Orion Bar, and NGC 2024 (Fig. 1*b*). Both the ^{13}CO and the ^{12}CO $J = 6 \rightarrow 5$ spectra taken on Θ^1C and the Bar are affected by emission in the reference beams (self-chopping) due to the

[1] Max-Planck-Institut für extraterrestrische Physik, Garching.
[2] Mullard Radio Astronomy Observatory, Cambridge.
[3] Joint Astronomy Centre, Hilo, Hawaii.

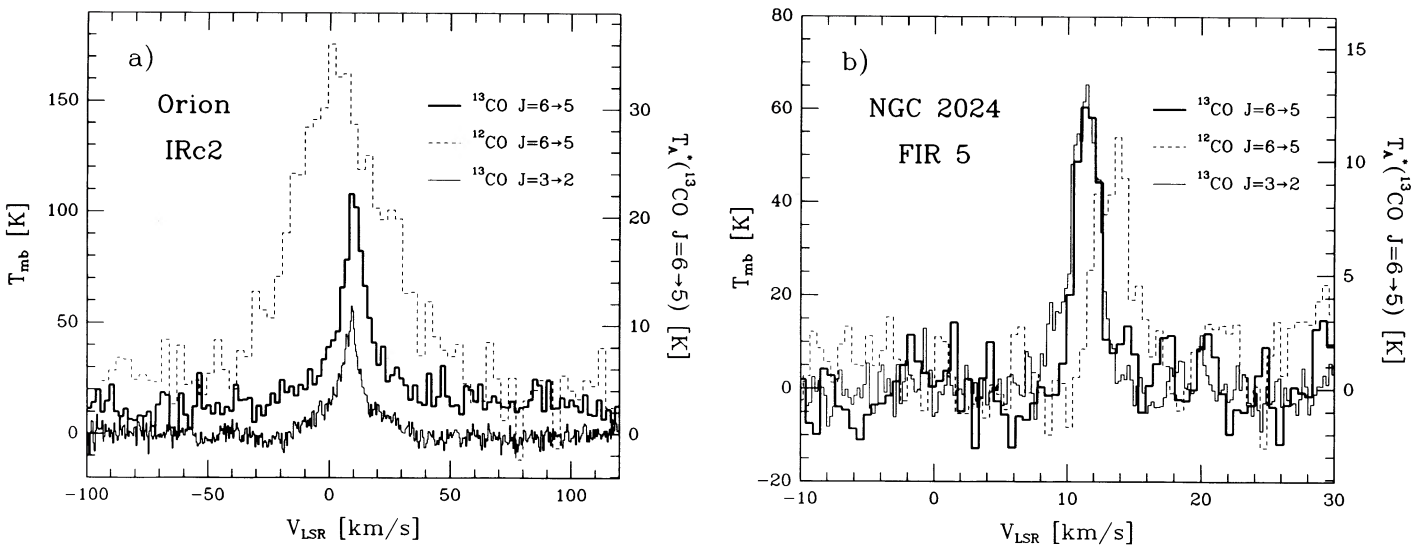

FIG. 1.—Overlay of CO lines detected toward (*a*) Orion IRc2 ($5^h32^m47^s.0$, $-5°24'23''$ [1950]) and (*b*) NGC 2024 (FIR 5, $5^h39^m12^s.8$, $-1°57'04''$ [1950] Mezger *et al.* 1988): ^{13}CO $J = 6 \rightarrow 5$ (*heavy solid line*), ^{12}CO $J = 6 \rightarrow 5$ (*dashed line*), and ^{13}CO $J = 3 \rightarrow 2$ (*light solid line*). The intensity scale is in units of Rayleigh-Jeans main beam brightness temperature. In addition, the T_A^* scale is given for the ^{13}CO $J = 6 \rightarrow 5$ line. No baseline corrections have been applied to the $6 \rightarrow 5$ spectra. A linear baseline has been subtracted from the $3 \rightarrow 2$ line. The ^{13}CO lines toward Orion are composed of two distinct components: a narrow "spike" component and a broader "plateau," while the ^{12}CO $J = 6 \rightarrow 5$ line is dominated by plateau emission and does not show the spike component. The velocity shift between the ^{13}CO lines and the main isotope in NGC 2024 is probably due to foreground absorption (Graf *et al.* 1990) in the optical dust lane (compare Barnes *et al.* 1989 who find OH absorption centered on 9 km s^{-1}).

limited chop throw of 120″. The intensities measured toward the Bar and Θ^1C are thus only lower limits to the source intensities. The ^{13}CO $J = 3 \rightarrow 2$ line, taken in position-switched mode, does not show self-chopping. In all sources observed, the ^{13}CO lines are narrower than the ^{12}CO $J = 6 \rightarrow 5$ line. Toward NGC 2023, no strong ^{13}CO $J = 6 \rightarrow 5$ emission was detected. Table 1 summarizes the observed line parameters.

III. DISCUSSION

The ^{13}CO $J = 6$ level lies 111 K above ground state. The $J = 6 \rightarrow 5$ transition has an A-coefficient of 1.9×10^{-5} s^{-1}, and in optically thin gas the critical density is $\approx 2 \times 10^5$ cm^{-3} (based on ^{12}CO collision rates given by Flower and Launay 1985). The high brightness temperature seen in this transition is an immediate proof of the presence of large amounts of warm, dense gas. In the optically thin limit, a typical integrated line intensity of 120 K km s^{-1} (NGC 2024) implies a ^{13}CO column density in the $J = 6$ level of 5×10^{15} cm^{-2}. Assuming LTE conditions, the maximum fractional population of the $J = 6$ level is $\approx 11\%$. This constrains the total column density in warm ^{13}CO to $\geq 5 \times 10^{16}$ cm^{-2}.

a) Radiative Transfer Modeling

We compared the results from an escape probability, radiative transfer program (Stutzki and Winnewisser 1985) with the observed source parameters (Fig. 2).

The ^{12}CO $J = 6 \rightarrow 5$ line profiles differ substantially from the isotopic $6 \rightarrow 5$ line (Fig. 1). The optically thick ^{12}CO $J = 6 \rightarrow 5$ emission does not trace the bulk of the warm molecular material. We therefore base our radiative transfer analysis on the ^{13}CO lines only, since these are likely to have only moderate optical depths. At $70 \leq T_{kin} \leq 400$ K and densities $\geq 10^5$ cm^{-3}, the ^{13}CO $6 \rightarrow 5/3 \rightarrow 2$ ratio is a good measure of the kinetic gas temperature (Fig. 2). The similarity of the ^{13}CO $6 \rightarrow 5$ and $3 \rightarrow 2$ line profiles supports the assumption that they arise from the same material. Nevertheless, a certain fraction of the $3 \rightarrow 2$ emission could come from cooler gas not traced by the higher energy $6 \rightarrow 5$ transition. The temperatures given

TABLE 1

LINE PARAMETERS[a]

Source	Line	T_{mb} (K)[b]	v_{LSR} (km s^{-1})	Δv (km s^{-1})
IRc2[d]:				
Spike	^{13}CO $6 \rightarrow 5$	64 ± 3	10.1 ± 0.1	7.7 ± 0.4
	^{13}CO $3 \rightarrow 2$	30 ± 1	8.9 ± 0.1	6.8 ± 0.2
Plateau	^{13}CO $6 \rightarrow 5$	31 ± 2	10.2 ± 0.6	32.8 ± 2.0
	^{13}CO $3 \rightarrow 2$	17 ± 0.5	8.8 ± 0.3	37.7 ± 1.5
	^{12}CO $6 \rightarrow 5$	133	3.9	44.2
Orion Bar[e]	^{13}CO $6 \rightarrow 5$	≥ 30[e]	≈ 9.0	≈ 3.0
	^{13}CO $3 \rightarrow 2$	22	10.0	4.0
NGC 2024[f]				
(0″, 0″)	^{13}CO $6 \rightarrow 5$	69	11.5	2.0
	^{13}CO $3 \rightarrow 2$	62	11.2	2.1
	^{12}CO $6 \rightarrow 5$	45	13.5	2.9
NGC 2024				
(−15″, 15″)	^{13}CO $6 \rightarrow 5$	57	11.3	2.0
	^{13}CO $3 \rightarrow 2$	38	11.1	2.2
NGC 2023[g]				
(60″, −60″)	^{13}CO $6 \rightarrow 5$	≤ 10	...	...
	^{12}CO $6 \rightarrow 5$	58	11.5	1.9

[a] From one- or two-component Gaussian fits.
[b] The errors quoted are formal 1 σ errors of the two-component fit and do not include systematic errors in the data.
[c] Lower limit because of self-chopping.
[d] $5^h32^m47^s.0$, $-5°24'23''$ (1950).
[e] $5^h32^m52^s.3$, $-5°27'01''$ (1950).
[f] $5^h39^m12^s.8$, $-1°57'04''$ (1950) (FIR 5; Mezger *et al.* 1988).
[g] $5^h39^m07^s.3$, $-2°16'58''$ (1950).

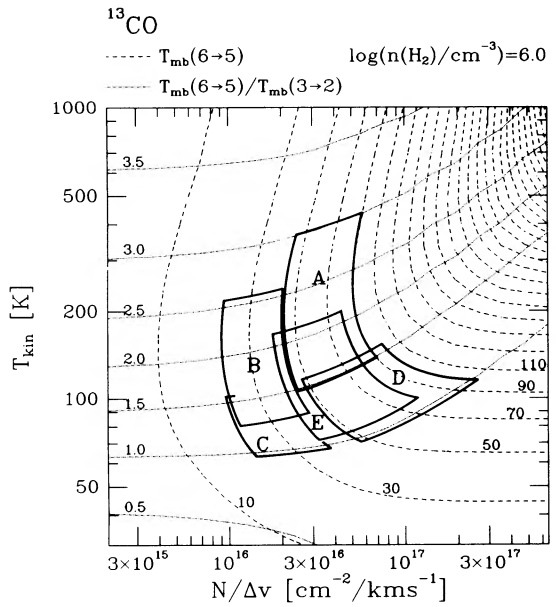

FIG. 2.—Radiative transfer model of the ^{13}CO emission compared with the observed source parameters. The model is calculated for an H_2 density of 10^6 cm^{-3}. We present the results in the two-dimensional parameter space spanned by the kinetic gas temperature and the ^{13}CO column density per velocity interval. The dashed lines are curves of constant ^{13}CO $J = 6 \rightarrow 5$ peak brightness temperatures; the dotted lines represent constant ratios of $6 \rightarrow 5/3 \rightarrow 2$ peak brightness temperatures. The heavy boxes outline the range of parameters consistent with the observed values for the individual sources: A, Orion IRc2 (spike); B, Orion IRc2 (plateau); C, Orion Bar (lower limits); D, NGC 2024 (0″, 0″); E, NGC 2024 (−15″, 15″).

below thus have to be considered as lower limits to the kinetic temperature of the gas emitting the ^{13}CO $J = 6 \rightarrow 5$ line.

The radiative transfer model results do not depend strongly on the particle density as long as it is close to or higher than the critical density of the CO transitions involved (a few times 10^5 cm^{-3}). As an example we show the case of a density of 10^6 cm^{-3} (Fig. 2; Table 2.) A variety of molecular line studies indicate that this is a typical density for the sources we consider here (Orion: Genzel, Poglitsch, and Stacey 1988 and Stacey *et al.* 1990; NGC 2024: Snell *et al.* 1984). For the observed range of brightness temperatures the column density is constrained by the intensity of the ^{13}CO $J = 6 \rightarrow 5$ emission to $4 \times 10^{16} \leq N(^{13}CO) \leq 5 \times 10^{17}$ cm^{-2}. The $6 \rightarrow 5/3 \rightarrow 2$ intensity ratio constrains the temperature to ≥ 100 K. Over this range of parameters the ^{13}CO $J = 6 \rightarrow 5$ line is still optically thin [$\tau \leq 0.6$, except for NGC 2024 (0, 0): $\tau \approx 1.5$]. The temperatures and column densities derived for the individual sources are listed in Table 2. The difference between the column densities found in the two NGC 2024 positions may be overestimated, as it results mainly from the difference in the $J = 3 \rightarrow 2$ line intensity. Toward the high column density clump FIR 5, it is likely that cooler gas contributes a significant fraction to the $3 \rightarrow 2$ intensity, thus producing an artificially low $6 \rightarrow 5/3 \rightarrow 2$ ratio.

b) Heating Mechanisms

The strong line emission detected in the ^{13}CO $J = 6 \rightarrow 5$ transition from both dynamically active and quiescent material confirms the presence of large amounts of warm, dense gas in star-forming regions. The intense and narrow lines observed in the Orion Bar and in NGC 2024 imply column densities of quiescent H_2 of several times 10^{22} cm^{-2} (Table 2). This amount of warm quiescent gas is difficult to explain by known heating mechanisms.

TABLE 2

DERIVED TEMPERATURES AND COLUMN DENSITIES[a]

Source	T_{kin} (K)	$N(^{13}CO)$[b] (cm^{-2})	$N(H_2)$[c] (cm^{-2})	$N_{tot}(H_2)$[d] (cm^{-2})
IRc2 (spike)	185	2.5(17)	2.1(23)	2.5(23)[f]
IRc2 (plateau)	120	4.6(17)	3.8(23)	≤1.0(23)[g]
Orion Bar	≥70	≥3.8(16)	≥3.2(22)	3.2(22)[h]
NGC 2024 (0″, 0″)	95	1.5(17)	1.3(23)	1.0(23)[i]
NGC 2024 (−15″, 15″)	115	6.8(16)	5.7(22)	1.0(23)[i]
NGC 2023[e]	85	<1.5(16)	<1.3(22)	5.6(22)[j]

[a] Fits to the line intensities and ratios from escape probability models with $n(H_2) = 10^6$ cm^{-3}.
[b] 2.5(17) = 2.5×10^{17}.
[c] Assumes $[^{12}CO]/[^{13}CO] = 67$ (Langer and Penzias 1990) and $[^{12}CO]/[H_2] = 8 \times 10^{-5}$.
[d] Total H_2 column densities derived from lower excitation lines, beam-averaged over 11″ to 1′.
[e] Fit to the ^{13}CO $J = 6 \rightarrow 5$ intensity from an escape probability radiative transfer model with $n(H_2) = 10^4$ cm^{-3}. Assumes $T_{kin} = 85$ K, $\Delta v_{LSR} = 1.5$ km s^{-1} (Jaffe *et al.* 1989).
[f] Wilson *et al.* 1986 (from $C^{18}O$ $J = 1 \rightarrow 0$ data, 21″ beam).
[g] Blake *et al.* 1987 (multiline study, ≈0.5 beam).
[h] Own $C^{18}O$ data, 11″ beam.
[i] Snell *et al.* 1984 (from CS $J = 2 \rightarrow 1, 3 \rightarrow 2, 5 \rightarrow 4, 6 \rightarrow 5$ data, ≈1′ beams).
[j] Jaffe *et al.* 1990 (from $C^{18}O$ $J = 2 \rightarrow 1$ data, 34″ beam).

i) *Shock Heating*

Shocks are probably the dominant heating mechanism in the Orion plateau source (Draine and Roberge 1982, 1984; Chernoff, Hollenbach, and McKee 1982) but are very unlikely to play a major role in the heating of the quiescent gas. The narrow line widths detected in NGC 2024 and the Orion Bar limit the shock velocity to a few km s^{-1}, unless the shocks are extremely well aligned perpendicular to the line of sight. Assuming densities and column densities similar to the ones we see in the Bar or NGC 2024, Draine and Roberge (1984) derive a line intensity of $\approx 4 \times 10^{-6}$ ergs cm^{-2} s^{-1} sr^{-1} in the $J = 6 \rightarrow 5$ transition of ^{12}CO for a shock velocity of 5 km s^{-1} and a magnetic field strength near 1 mG. This is about 10 times lower than the intensity seen in the isotopic ^{13}CO $J = 6 \rightarrow 5$ line toward NGC 2024. The $6 \rightarrow 5$ emission in the Draine and Roberge (1984) model is optically thin. Thus, assuming $[^{12}CO]/[^{13}CO] = 67$ (Langer and Penzias 1990), $10 \times 67 \approx 700$ shock fronts are required along the line of sight to add up to the observed intensity. With the observed lines being even narrower than the assumed shock velocity of 5 km s^{-1}, it seems extremely unlikely that any shocks described by currently available models are an important heat source in the warm, quiescent gas.

ii) *Dust-Gas Collisional Heating*

At densities of $\geq 10^6$ cm^{-3} thermal coupling by collisions between the gas and the dust becomes important. The cooling rate from the observed ^{13}CO $J = 6 \rightarrow 5$ emission in NGC 2024 is $\approx 10^{-20}$ ergs s^{-1} cm^{-3}. Summing over all ^{13}CO lines increases this cooling rate by about a factor of 10. We estimate

that the energy loss by the optically thick ^{12}CO lines is about twice as high as that due to ^{13}CO, resulting in a total cooling rate in all CO lines of $\approx 3 \times 10^{-19}$ ergs s^{-1} cm^{-3}. To balance this energy loss by dust-gas collisional heating would require a dust temperature of ≈ 115 K, assuming a gas temperature of 100 K and an H_2 density of 10^6 cm^{-3} (Black 1987). Taking into account the T^5 dependence of the thermal emission of a gray body, it seems unlikely that a substantial fraction of the dust can have temperatures ≥ 100 K. Values closer to the observed dust temperatures of 50–60 K (NGC 2024: Gordon 1988 and Thronson *et al.* 1984) would imply a kinetic gas temperature of ≈ 40 K. This would only be consistent with the observations presented here, if both lines entering in the radiative transfer model were miscalibrated by a factor of 2, and if all of the ^{13}CO $J = 3 \rightarrow 2$ emission came from the warm gas component (see § III*a*).

iii) *Photoheating*

Photodissociation regions (PDRs) formed at the surface of molecular clouds exposed to far-UV radiation (Tielens and Hollenbach 1985; Sternberg and Dalgarno 1989) can account for the mid-J ^{12}CO line emission from sources of lower UV flux and lower density (NGC 2023: Jaffe *et al.* 1990, Table 1) but do not produce the high column densities of warm gas we observed in NGC 2024 and the Orion Bar. Higher column densities of warm CO may be produced in dense ($\geq 10^6$ cm^{-3}) PDRs (Burton, Hollenbach, and Tielens 1990; Sternberg 1990). In such regions the high CO formation rate increases the amount of warm CO, and, due to the high density, the mid-J level populations become thermalized. In a PDR with $n = 10^6$ cm^{-3} exposed to a UV field 10^5 times more intense than the average interstellar radiation field, for instance, the predicted intensity of the ^{12}CO $J = 6 \rightarrow 5$ transition is ≈ 165 K km s^{-1}. The same model predicts a ^{13}CO $J = 6 \rightarrow 5$ line intensity of only 14 K km s^{-1}. If the observed narrow ^{13}CO $J = 6 \rightarrow 5$ emission lines are formed in PDRs, the effective UV absorption cross section per hydrogen nucleus of the dust grains must be unusually small ($\approx 10^{-22}$ cm^2 at 1000 Å) in order to allow the UV radiation to heat the gas to an H_2 column density of a few times 10^{22} cm^{-2} (Sternberg 1990).

We thank the staff of the JCMT for their excellent support during the observing run. JCMT is operated by the Royal Observatory, Edinburgh, on behalf of the UK Science and Engineering Research Council, the Netherlands Organisation for Pure Research and the National Research Council of Canada. We are grateful to A. Sternberg for valuable discussions and to R. Densing who provided the output coupler for the new FIR laser line.

REFERENCES

Arimondo, E. 1984, in *Reviews of Infrared and Millimeter Waves*, Vol. **2**, *Optically Pumped Far-Infared Lasers*, ed. K. J. Button, M. Inguscio, F. Strumia (New York: Plenum Press), p. 81.
Barnes, P. J., Crutcher, R. M., Bieging, J. H., Storey, J. W. V., and Willner, S. P. 1989, *Ap. J.*, **342**, 883.
Boreiko, R. T., Betz, A. L., and Zmuidzinas, J. 1989, *Ap. J.*, **337**, 332.
Black, J. H. 1987, in *Interstellar Processes*, ed. D. J. Hollenbach and H. A. Thronson, Jr. (Dordrecht: Reidel), p. 731.
Blake, G. A., Sutton, E. C., Masson, C. R., and Phillips, T. G. 1987, *Ap. J.*, **315**, 621.
Burton, M., Hollenbach, D., and Tielens, A. G. G. M. 1989, in *Infrared Spectroscopy in Astronomy*, ed. B. H. Kaldeich (Noordwijk: ESA Publications Division), p. 141.
Chernoff, D. F., Hollenbach, D. J., and McKee, C. F. 1982, *Ap. J.*, **259**, L97.
Draine, B. T., and Roberge, W. G. 1982, *Ap. J. (Letters)*, **259**, L91.
———. 1984, *Ap. J.*, **282**, 491.
Dyubko, S. F., Fesenko, L. D., Baskakov, O. I., and Svich, V. A. 1975, *Zh. Prikl. Spektrosk.*, Vol. **23**, No. 2, p. 317.
Dyubko, S. F., Svich, A. V., and Fesenko, L. D. 1975, *Zh. Tekh. Fiz.*, **45**, 2458.
Flower, D. R., and Launay, J. M. 1985, *M.N.R.A.S.*, **214**, 271.
Genzel, R., Poglitsch, A., and Stacey, G. J. 1988, *Ap. J. (Letters)*, **333**, L59.
Graf, U. U., *et al.* 1990, in preparation.
Gordon, M. A. 1988, *Ap. J.*, **331**, 509.
Harris, A. I. 1986, Ph.D. thesis, University of California, Berkeley.
Harris, A. I., Jaffe, D. T., Stutzki, J., and Genzel, R. 1987*a*, *Internat. J. Infrared Millimeter Waves*, Vol. **8**, No. 8, p. 587.
Harris, A. I., Stutzki, J., Genzel, R., Lugten, J. B., Stacey, G. J., and Jaffe, D. T. 1987*b*, *Ap. J. (Letters)*, **322**, L49.
Jaffe, D. T., Genzel, R., Harris, A. I., Howe, J. E., Stacey, G. J., and Stutzki, J. 1990, *Ap. J.*, **353**, 193.
Jaffe, D. T., Harris, A. I., and Genzel, R. 1987, *Ap. J.*, **316**, 231.
Langer, W. D., and Penzias, A. A. 1990, *Ap. J.*, **357**, 477.
Lovas, F. J., and Krupenie, P. H. 1974, *J. Phys. Chem. Ref. Data*, Vol. **3**, No. 1, p. 245.
Mezger, P. G., Chini, R., Kreysa, E., Wink, J. E., and Salter, C. J. 1988, *Astr. Ap.*, **191**, 44.
Schmid-Burgk, J., *et al.* 1989, *Astr. Ap.*, **215**, 150.
Snell, R. L., Mundy, L. G., Goldsmith, P. F., Evans, N. J., and Erickson, N. R. 1984, *Ap. J.*, **276**, 625.
Sternberg, A. 1990, in preparation.
Sternberg, A., and Dalgarno, A. 1989, *Ap. J.*, **338**, 197.
Stacey, G. J., *et al.* 1990, in preparation.
Stutzki, J., and Winnewisser, G. 1985, *Astr. Ap.*, **148**, 254.
Tielens, A. G. G. M., and Hollenbach, D. 1985, *Ap. J.*, **291**, 722.
Thronson, H. A., Jr., Lada, C. J., Schwartz, P. R., Smith, H. A., Smith, J., Glaccum, W., Harper, D. A., and Loewenstein, R. F. 1984, *Ap. J.*, **280**, 154.
Wilson, T. L., Serabyn, E., Henkel, C., and Walmsley, C. M. 1986, *Astr. Ap.*, **158**, L1.

R. GENZEL, U. U. GRAF, A. I. HARRIS, A. P. G. RUSSELL, and J. STUTZKI: Max-Planck-Institut für Physik und Astrophysik, Institut für Extraterrestrische Physik, D-8046 Garching bei München, Federal Republic of Germany

R. E. HILLS: Mullard Radio Astronomy Observatory, Cavendish Laboratory, Maddingley Road, Cambridge CB3 0HE, United Kingdom